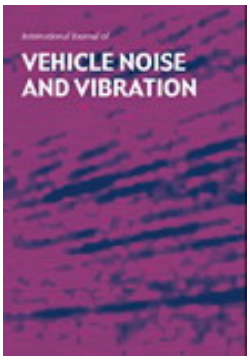

International Journal of Vehicle Noise and Vibration

ISSN online: 1479-148X - ISSN print: 1479-1471
https://www.inderscience.com/ijvnv

Decoupling optimisation of 12-degree-of-freedom mount system

Zhihong Lin, Dezhao Lin, Di Gong, Yunxiao Chen, Mingzhong Wu

DOI: 10.1504/IJVNV.2022.10050576

Article History:

Received:	24 May 2021
Accepted:	09 August 2021
Published online:	16 September 2022

Decoupling optimisation of 12-degree-of-freedom mount system

Zhihong Lin*

College of Intelligent Manufacturing,
Xiamen City University,
Xiamen Fujian 361008, China
Email: lin123hongzhi@163.com
*Corresponding author

Dezhao Lin, Di Gong, Yunxiao Chen and Mingzhong Wu

College of Mechanical Engineering and Automation,
HuaQiao University,
Xiamen, 361021, China
Email: lin_dezhao@foxmail.com
Email: di_gong@foxmail.com
Email: chenyx@stu.hqu.edu.cn
Email: jdwmz62@hqu.edu.cn

Abstract: To solve the vibration problem caused by the coupling of the powertrain and the mount system composed of the vehicle frame, the 12-degree-of-freedom mount system is used as the research object. Firstly, the natural frequency, decoupling rate and powertrain displacement response of the 6 and 12 degrees of freedom mount systems are solved. Secondly, the spectral radius of the coupling matrix of the 12-degree-of-freedom mount system is solved. The coupling matrix is shown to converge, and the vehicle frame centre-of-mass displacement response equation is solved by the coupling matrix without considering the road excitation. Finally, a multi-objective genetic algorithm is used to optimise the mount system with the maximum decoupling rate and the minimum vehicle centre-of-mass displacement response as the optimisation objectives. The numerical values show that the decoupling optimisation method better solves the coupling problem of the mount system and decreases the powertrain and vehicle frame displacement vibration response.

Keywords: 6 degrees of freedom; 12 degrees of freedom; mount system; multi-objective genetic algorithm.

Reference to this paper should be made as follows: Lin, Z., Lin, D., Gong, D., Chen, Y. and Wu, M. (2022) 'Decoupling optimisation of 12-degree-of-freedom mount system', *Int. J. Vehicle Noise and Vibration*, Vol. 18, Nos. 1/2, pp.1–21.

Biographical notes: Zhihong Lin is currently working at the College of Intelligent Manufacturing, Xiamen City University, China. He graduated from Huaqiao University with a PhD in Mechanical Engineering. He received his MS in Marine and Offshore Engineering from Jimei University. His research interests include control, dynamics, and vehicle NVH.

Dezhao Lin is a PhD candidate at the Huaqiao University. He obtained his BSc and MSc in the College of Mechanical Engineering and Automation of Huaqiao University, Xiamen, Fujian, China in 2017 and 2020. His current research project is focusing on vibration control and vehicle suspension.

Di Gong is a PhD student at the Huaqiao University. He received his BSc in Mechanical Engineering from the Shanghai University in 2016. His current research project includes magneto-active elastomers and magnetorheological elastomers and their applications.

Yunxiao Chen is a PhD candidate at Huaqiao University. He obtained his MSc in College of Computer Science of Huaqiao University. His current research project is focusing on robotics control.

Mingzhong Wu is a PhD candidate College of Mechanical, Electrical and Automation, Huaqiao University, Xiamen, China. Now, he works at Xiamen. His current research interests include vibration and control.

1 Introduction

The development of the automotive industry and the light weighting of automobiles have brought more serious problems of automotive vibration and noise (Wang, 2010). Engine reciprocating inertial force excitation and road excitation, while the vehicle is running, are the main sources of vehicle vibration (Lee and Choi, 1981). How to cope with the light weighting of automobiles and design a high-performance powertrain mount system. Effectively solving the problem of increased vibration and deterioration of NVH quality has become an important issue and an urgent need to improve the NVH quality of automobiles. The vibration isolation characteristics of the powertrain mount system directly affect the ride comfort of the vehicle. And a favourable engine mounts system can reduce the transmission of vibration to the vehicle frame, reduce interior noise, improve ride comfort, and at the same time well protect the powertrain (Swanson, 1993). By component type powertrain mounts can be divided into rubber mounts, hydraulic mounts, and by control method passive, semi-active and active mounts (Rivin, 1985; Mita and Ushijima, 1986; Yoon and Singh, 2011). However, a multi-degree-of-freedom powertrain mount system has inter-coupling effects. Therefore, decoupling optimisation of the mount system and improving the mount system vibration isolation are means to improve the NVH of the vehicle (Michael, 1994; Takano and Kojima, 1988; Colgate et al., 1995). Mount system decoupling is studied for 6-degree-of-freedom decoupling without considering vehicle frame influence, and the other one is 12-degree-of-freedom system decoupling considering vehicle frame influence. The decoupled optimal design of the 6-degree-of-freedom powertrain mount system assumes that the mounts are connected on a rigid basis. Qatu (2012) developed the dynamics equations of a 6-degree-of-freedom powertrain mount system to optimise the design of the three-way stiffness. Moreover, it is experimentally verified that the powertrain NVH performance is improved under the engine idle condition excitation. Erdelyi et al. (2013) proposed a method for decoupling

the coupling problem of rigid frame mode mount systems in torque axis systems, and implemented in the corresponding software by the proposed method. Sun and Jin (2012) developed a 6-degree-of-freedom dynamics model of the bus powertrain mount system for the bus vibration problem. With the objective of maximising the decoupling rate of the 6-degree-of-freedom mount system, the energy decoupling theory is used to optimise the mount system. Jeong (2000) proposed the TRA decoupling condition for the powertrain rubber mount undamped system based on the torque axis (TRA) decoupling principle, and the decoupling condition was verified analytically. For the engine vibration problem caused by idle speed, TRA decoupling based on a 6-degree-of-freedom mount system is used to effectively solve the vibration problem caused by engine torque excitation (Dai et al., 2013; Erdelyi et al., 2013; Park and Singh, 2007). The decoupling theory of 6-degree-of-freedom powertrain mount system is based on the fact that the mount connection is on a rigid basis, ignoring the interactions between other subsystems. Considering the decoupling of a 12-degree-of-freedom system with vehicle elasticity is a theoretical extension and complement to the 6-degree-of-freedom. Hu and Singh (2012) analysed the effect of the vehicle frame on the decoupling of the torque axis from the perspective of the eigen solution and frequency response based on the conditions for decoupling of the torque axis proposed by Jeong and Singh. Then, the mathematical formula is derived to solve the complete decoupling of the torque axis considering the vehicle frame. Wu et al. (2018) used a robust design approach using Isight and MATLAB to decouple and optimise a 12-degree-of-freedom mount system based on Hu's theory of complete decoupling of the torque axes considering the vehicle frame. Lee et al. (1995) discussed the effect of flexible foundations on the force response of powertrain mount systems. Then, the modal information obtained from finite element analysis or experimental modal analysis is used to represent the dynamic elasticity of the foundation. By solving the derived equations, the natural frequency and forced vibration response of the powertrain mount system are accurately simulated. There are also studies on vibration isolation of suspension systems from the control point of view. These include Mahil and Faris (2014) vibration isolation control study of a 6-degree-of-freedom mount system using integral derivative (PID) and linear quadratic regulator (LQR), respectively.

In summary, the decoupling optimisation theories for both 6 and 12 degrees of freedom mount systems are relatively mature. However, this study focuses on the powertrain response and ignores the vehicle frame vibration response. The specific research objectives of this paper are as follows:

1 Derive mathematical equations for 6 and 12 degrees of freedom mount systems, respectively, and compare the effect of considering the vehicle frame elasticity problem on the mount system or not.

2 Solve the coupling equation of powertrain and vehicle frame, and solve the vehicle displacement response by the coupling equation.

3 A multi-objective genetic algorithm is used to optimise the design of the 12-degree-of-freedom mount system with the maximum decoupling rate in the first six orders and the minimum frame displacement response.

2 6 degrees of freedom and 12 degrees of freedom mount system formula derivation

2.1 6-degree-of-freedom mount system

Assume the generalised coordinates q^e of the powertrain, where x^p, y^p, and z^p denote the powertrain moving flat along the coordinate axis and θ_x^p, θ_y^p and θ_z^p denote the powertrain rotating around the coordinate axis, respectively. In this study, the number of mounts n = 3, and the established 6-degree-of-freedom mount system is shown in Figure 1.

Figure 1 6-degree-of-freedom mount system (see online version for colours)

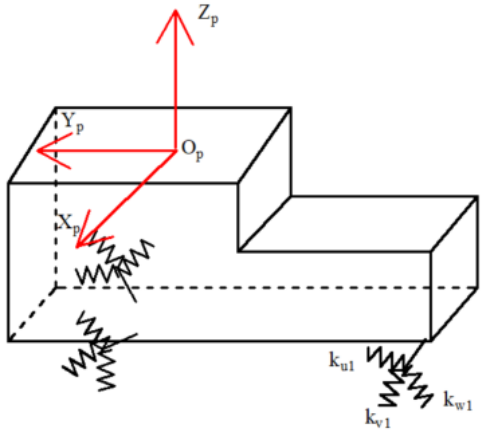

The local stiffness K_{mi} and damping C_{mi} of the i^{th} mounts in the three principal axis directions are:

$$K_{mi} = \begin{bmatrix} k_{ui} & 0 & 0 \\ 0 & k_{vi} & 0 \\ 0 & 0 & k_{wi} \end{bmatrix}, C_{mi} = \begin{bmatrix} c_{ui} & 0 & 0 \\ 0 & c_{vi} & 0 \\ 0 & 0 & c_{wi} \end{bmatrix} \tag{1}$$

With the known angle between the local coordinate system of the mounts and the powertrain coordinate system, the stiffness matrix K_{mi} and the damping matrix C_{mi} of the local mounts can be converted into the powertrain coordinate system through the rotation matrix T. From them, the stiffness matrix and the damping matrix of the mount in the powertrain coordinate system are obtained.

$$K_i = TK_{mi}T^T = \begin{bmatrix} k_{xx} & k_{xy} & k_{xz} \\ k_{xy} & k_{yy} & k_{yz} \\ k_{xz} & k_{yz} & k_{zz} \end{bmatrix}, C_i = TC_{mi}T^T = \begin{bmatrix} c_{xx} & c_{xy} & c_{xz} \\ c_{xy} & c_{yy} & c_{yz} \\ c_{xz} & c_{yz} & c_{zz} \end{bmatrix} \tag{2}$$

Since the mounts are directly connected to the ground, the displacement of the i^{th} mount is $q_i^e(t)$ can be expressed by the powertrain displacement $q^e(t)$. Therefore, the

translational displacement of the i^{th} mount is $q_i^e(t) = x^p + y^p + z^p + (\theta_x^p + \theta_y^p + \theta_z^p) \times P_i^e$. Where P_i^e is solved as shown below,

$$P_i^e = \begin{bmatrix} 1 & 0 & 0 & 0 & z_i^e & -y_i^e \\ 0 & 1 & 0 & -z_i^e & 0 & x_i^e \\ 0 & 0 & 1 & y_i^e & -x_i^e & 0 \end{bmatrix} \tag{3}$$

where x_i^e, y_i^e, z_i^e are the positions of the i^{th} mount relative to the centre-of-mass of the powertrain.

Based on the above derivation, the force $f_i^e(t)$ and moment $T_i^e(t)$ acting on the powertrain for the i^{th} mount are:

$$f_i^e(t) = -K_i P_i^e q^e(t) \tag{4}$$

$$T_i^e(t) = A_i^e f_i^e(t) \tag{5}$$

where

$$A_i^e = \begin{bmatrix} 0 & z_i^e & -y_i^e \\ -z_i^e & 0 & x_i^e \\ y_i^e & -x_i^e & 0 \end{bmatrix} \tag{6}$$

The final solved vibration equation (7) for the powertrain mount system is shown.

$$M_e \ddot{q}^e(t) + C_e \dot{q}^e(t) + K_e q^e(t) = f^e(t) \tag{7}$$

where

$$M_e = \begin{bmatrix} m^e & 0 & 0 & 0 & 0 & 0 \\ 0 & m^e & 0 & 0 & 0 & 0 \\ 0 & 0 & m^e & 0 & 0 & 0 \\ 0 & 0 & 0 & I_{xx}^e & -I_{xy}^e & -I_{xz}^e \\ 0 & 0 & 0 & -I_{xy}^e & I_{yy}^e & -I_{yz}^e \\ 0 & 0 & 0 & -I_{xz}^e & -I_{yz}^e & I_{zz}^e \end{bmatrix} \tag{8}$$

$$K^e = \sum_{i=1}^{3} P_i^{eT} K_i P_i^e, C^e = \sum_{i=1}^{3} P_i^{eT} C_i P_i^e \tag{9}$$

2.2 12-degree-of-freedom mount system

The 12-degree-of-freedom mount system is shown in Figure 2, where the elastic base consists of a rigid vehicle frame and four bushings. Assuming the generalised coordinates $q^c(t) = [x^b \quad y^b \quad z^b \quad \theta_x^b \quad \theta_y^b \quad \theta_z^b]$ of the vehicle frame, the equations x^b, y^b, and z^b indicate that the vehicle frame is moving flat along the coordinate axis and θ_x^b, θ_y^b, and θ_z^b indicate that the vehicle frame is rotating around the coordinate axis, respectively.

Assume that the i^{th} suspension acts on the vehicle frame with force $f_i^b(t)$ and moment $T_i^b(t)$. The vibration equation of the mount system considering the vehicle frame base is obtained as follows.

$$M_c\ddot{q}^c(t)+C^c\dot{q}^c(t)+K^cq^c+K^{cl}q^c(t)+C^{cl}\dot{q}^c(t)=f^c(t) \tag{10}$$

where M_c is the mass matrix of the vehicle, K^{c1} and C^{c1} denote the stiffness matrix and damping matrix of the vehicle caused by the mounts, respectively, and x_i^b, y_i^b, z_i^b denote the relative coordinates of the i^{th} mount to the centre-of-mass of the vehicle. Where the expressions M_c, K^{c1}, C^{c1} are shown below.

$$K^{c1}=\sum_{i=1}^{3}P_i^{cT}K_iP_i^c,\ C^{c1}=\sum_{i=1}^{3}P_i^{cT}C_iP_i^c \tag{11}$$

$$P_i^c=\begin{bmatrix}1&0&0&0&z_i^b&-y_i^b\\0&1&0&-z_i^b&0&x_i^b\\0&0&1&y_i^b&-x_i^b&0\end{bmatrix} \tag{12}$$

$$M_c=\begin{bmatrix}m^c&0&0&0&0&0\\0&m^c&0&0&0&0\\0&0&m^c&0&0&0\\0&0&0&I_{xx}^c&-I_{xy}^c&-I_{xz}^c\\0&0&0&-I_{xy}^c&I_{yy}^c&-I_{yz}^c\\0&0&0&-I_{xz}^c&-I_{yz}^c&I_{zz}^c\end{bmatrix} \tag{13}$$

Figure 2 12-degree-of-freedom mount system (see online version for colours)

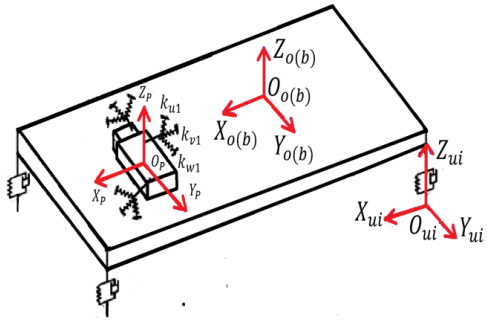

Solve for the forces $f_i^e(t)$, $f_i^c(t)$ acting on the powertrain and vehicle frame for the i^{th} mount according to Figure 2.

$$f_i^e(t)=-K_iP_i^eq^e(t)-C_iP_i^eq^e(t)+K_iP_i^cq^c(t)+C_iP_i^cq^c(t) \tag{14}$$

$$f_i^c(t)=-K_iP_i^cq^c(t)-C_iP_i^cq^c(t)+K_iP_i^eq^e(t)+C_iP_i^eq^e(t) \tag{15}$$

The moments $T_i^e(t), T_i^c(t)$ of the i^{th} mount acting on the powertrain and the vehicle frame.

$$T_i^e(t) = -A_i^e K_i P_i^e q^e(t) - A_i^e C_i P_i^e q^e(t) + A_i^c K_i P_i^c q^c + A_i^c C_i P_i^c q^c(t) \tag{16}$$

$$T_i^c(t) = -A_i^c K_i P_i^c q^c(t) - A_i^c C_i P_i^c q^c(t) + A_i^e K_i P_i^e q^e(t) + A_i^e C_i P_i^e q^e(t) \tag{17}$$

where

$$A_i^c = \begin{bmatrix} 0 & z_i^b & -y_i^b \\ -z_i^b & 0 & x_i^b \\ y_i^b & -x_i^b & 0 \end{bmatrix} \tag{18}$$

The local stiffness matrix k_c and the damping matrix c_c for the four bushings in vehicle frame coordinates are solved as follows.

$$K_k^c = P_{ik}^c k_c P_{ik}^{b^T},\ C_k^c = P_{ik}^c c_c P_{ik}^{b^T},\ K^c = \sum_{k=1}^{4} K_k^c,\ C^c = \sum_{k=1}^{4} C_k^c$$

where $x_{ik}^b, y_{ik}^b, z_{ik}^b$ denote the relative coordinates of the i^{th} bushing with respect to the centre-of-mass of the vehicle frame.

$$P_{ik}^c = \begin{bmatrix} 1 & 0 & 0 & 0 & z_{ik}^b & -y_{ik}^b \\ 0 & 1 & 0 & -z_{ik}^b & 0 & x_{ik}^b \\ 0 & 0 & 1 & y_{ik}^b & -x_{ik}^b & 0 \end{bmatrix} \tag{19}$$

$$k_c = \begin{bmatrix} k_{xi} & 0 & 0 \\ 0 & k_{yi} & 0 \\ 0 & 0 & k_{zi} \end{bmatrix},\ c_c = \begin{bmatrix} c_{xi} & 0 & 0 \\ 0 & c_{yi} & 0 \\ 0 & 0 & c_{zi} \end{bmatrix} \tag{20}$$

According to the above equation, the vibration equation of the 12-degree-of-freedom mount system can be obtained as:

$$M\ddot{q}(t) + C\dot{q}(t) + Kq(t) = f(t) \tag{21}$$

where $K^{e\to c}$, $C^{e\to c}$, $K^{c\to e}$, $C^{c\to e}$ are the coupling stiffness matrix and damping matrix between powertrain and vehicle frame; $f^e(t)$, $f^c(t)$ are the engine excitation and road excitation. The matrices M, C, K are shown below.

$$M = \begin{bmatrix} M_e & 0 \\ 0 & M_c \end{bmatrix},\ C = \begin{bmatrix} C^e & -C^{e\to c} \\ -C^{c\to e} & C^c + C^{c1} \end{bmatrix},\ K = \begin{bmatrix} K^e & -K^{e\to c} \\ -K^{c\to e} & K^c + K^{c1} \end{bmatrix} \tag{22}$$

$$K^{e\to c} = K^{c\to e} = \sum_{i=1}^{3} P_i^{e^T} K_i P_i^c,\ C^{e\to c} = C^{e\to e} = \sum_{i=1}^{3} P_i^{e^T} C_i P_i^c \tag{23}$$

$$f(t) = \begin{bmatrix} f^e(t) \\ f^c(t) \end{bmatrix} \tag{24}$$

3 Characteristic analysis of 6-degree-of-freedom and 12-degree-of-freedom mount system

3.1 Mount system parameters

The parameters of the 12-degree-of-freedom mount system include the powertrain centre-of-mass coordinates, mass and inertia parameters, the coordinates, stiffness and mounting angles of each mount in the overall vehicle coordinate system, the frame centre-of-mass coordinates, the mass and inertia parameters of the frame, and the stiffness and damping of the four bushings.

Table 1 Powertrain and vehicle frame related mass and inertia parameters

Name	*m (kg)*	I_{xx} *(kg.m²)*	I_{yy} *(kg.m²)*	I_{zz} *(kg.m²)*	I_{xz} *(kg.m²)*	I_{xy} *(kg.m²)*	I_{yz} *(kg.m²)*
Powertrain	168.8	14.036	5.8191	10.579	0.428	0.394	0.155
Car body	892.2	264.7	1658.5	2219	–253.2	235	226.40

Table 2 Position of powertrain centre-of-mass, vehicle frame centre-of-mass and each mount in vehicle coordinates

Coordinate	*Powertrain mass centre*	*Body mass centre*	*Left mount*	*Right mount*	*Rear mount*
X	1,400	0	1,090.1	1,983.4	272.4
Y	–20	0	–150.2	–72.7	337.6
Z	140	0	355.8	174.1	–114.1

Table 3 Installation angle of each mount (deg)

Local coordinates	*Left mount*			*Right mount*			*Rear mount*		
	X	*Y*	*Z*	*X*	*Y*	*Z*	*X*	*Y*	*Z*
U	0	90	–90	0	90	–90	0	90	–90
V	–90	0	90	–90	0	90	–90	0	90
W	90	–90	0	90	–90	0	90	–90	0

Table 4 Installation position and stiffness of each bushing

Bushing	*X/mm*	*Y/mm*	*Z/mm*	*Stiffness/(N/mm)*
Left front bushing	538.80	–748.30	22.80	21.20 (X, Y, Z)
Right front bushing	538.80	748.30	22.80	21.20 (X, Y, Z)
Left rear bushing	3,041.10	–741.50	–3.44	20.20 (X, Y, Z)
Right rear bushing	3,041.10	741.50	–3.44	20.20 (X, Y, Z)

3.2 Natural frequency and decoupling rate calculation

Damping is generally not considered when solving for the natural frequency of the powertrain mount system, so equations (7) and (21) are simplified to an undamped vibration system with the following vibration equations, respectively.

$$M_e\ddot{q}^e(t) + K^e q^e(t) = 0 \tag{25}$$

$$M\ddot{q}(t) + Kq(t) = 0 \tag{26}$$

The natural circular frequencies of the 6-degree-of-freedom and 12-degree-of-freedom mount systems can be obtained from $[K^{(e)} - \omega^2 M] = 0$. Assuming that the solutions of equations (25) and (26) can be expressed as then the principal vibration type A of the 6 and 12 degrees of freedom mount systems can be obtained from equation (27) as follows:

$$\left[K^{(e)} - \omega_i^2 M\right] A = 0 \tag{27}$$

In this paper, the decoupling rate of each order of the mount system is calculated using the energy decoupling method. When the 6-degree-of-freedom system consisting of the rigid frame of the powertrain and the elastomer of the mount system vibrates at the i^{th} order natural frequency, the kinetic energy assigned to the k^{th} generalised coordinate is:

$$T_k = \frac{1}{2}\omega_i^2 m_{kl} (\phi)_l (\phi)_k \tag{28}$$

where

ω the i^{th} order natural frequency of the system

m_{kl} the mass matrix of the mount system in its k rows and l columns elements

ϕ_i the i^{th} order formation of the mount system

$(\phi_i)_l(\phi_i)_k$ the l^{th} element and the k^{th} element of the i^{th} order formation of the mount system.

Then define the kinetic energy assigned to the mount system at the k^{th} generalised coordinate as a percentage of the total kinetic energy of the system as:

$$T = \frac{\sum_{k=1}^{12(6)} m_{kl} (\phi)_l (\phi)_k}{\sum_{l=1}^{12(6)} \sum_{k=1}^{12(6)} m_{kl} (\phi)_l (\phi)_k} \times 100\% \tag{29}$$

The total kinetic energy at each order of the natural frequency in the mount system is 100%, and the range of values of T is 0~100%. If the value of T_i is 100%, the corresponding i^{th} order mount system is completely decoupled.

3.3 With or without considering the influence of the vehicle frame on the characteristics of the mount system

According to equation (28), the natural frequencies and decoupling rates of the 6 and 12 degrees of freedom mount systems are obtained and compared as shown in Figures 3 and 4, respectively.

Figure 3 Natural frequencies of 6 and 12 degrees of freedom mount systems (see online version for colours)

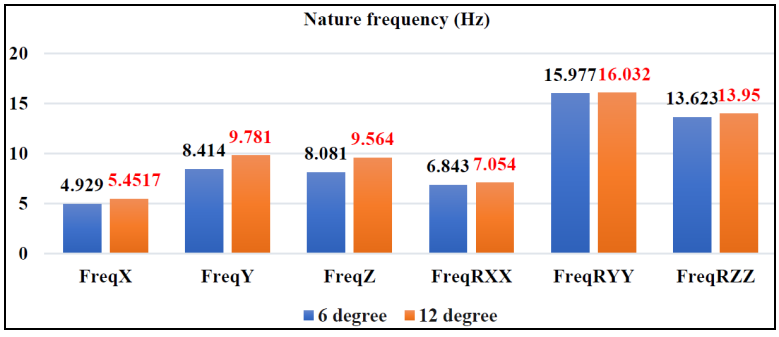

Figure 4 Decoupling rate of 6 and 12 degrees of freedom mount systems (see online version for colours)

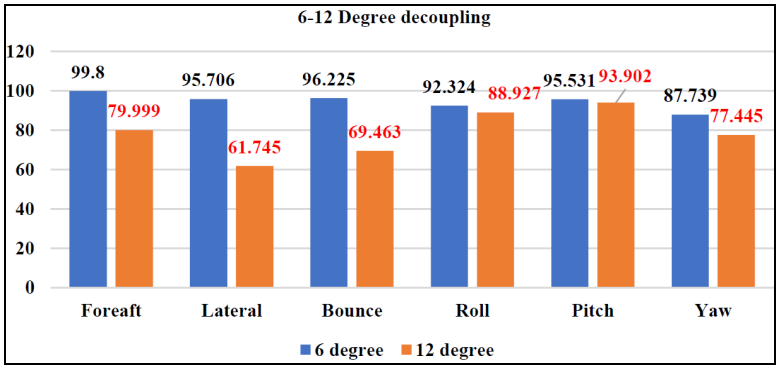

From Figure 3, it can be seen that the 6-degree-of-freedom and 12-degree-of-freedom powertrain mount systems have the greatest influence in the Z-direction and Y-direction. The natural frequencies of the 6-degree-of-freedom mount system in the Y-direction and Z-direction are 8.414 Hz and 8.081 Hz, respectively, while the natural frequencies of the 12-degree-of-freedom mount system considering the role of the vehicle frame increase to 9.781 Hz and 9.564 Hz in the Y-direction and Z-direction, respectively, with an increase of 16.25% and 18.35%. Figure 3 shows that considering the effect of the vehicle frame, the natural frequency of the mount system in the other four directions also has a corresponding increase, but the effect is less than the Y and Z directions. Similarly, Figure 4 shows that the 6-degree-of-freedom mount system has a high decoupling rate at all orders. However, the coupling between the orders of the 12-degree-of-freedom mount system considering the vehicle frame is very severe. In the same conclusion as in Figure 3, the 12-degree-of-freedom mount system considering the vehicle frame influence has the highest degree of coupling in the Y and Z directions, with the decoupling rate decreasing from 95.706% to 61.745 in the Y-direction and from 96.225% to 69.463% in the Z-direction. The decoupling rate of the other four directions in the mount system considering the influence of the vehicle frame also decreases accordingly. As a result, the vehicle frame has a significant impact on the natural characteristics and decoupling rate of the mount system.

Figure 5 Analysis of frequency response function of 6-degree-of-freedom and 12-degree-of-freedom mount system (see online version for colours)

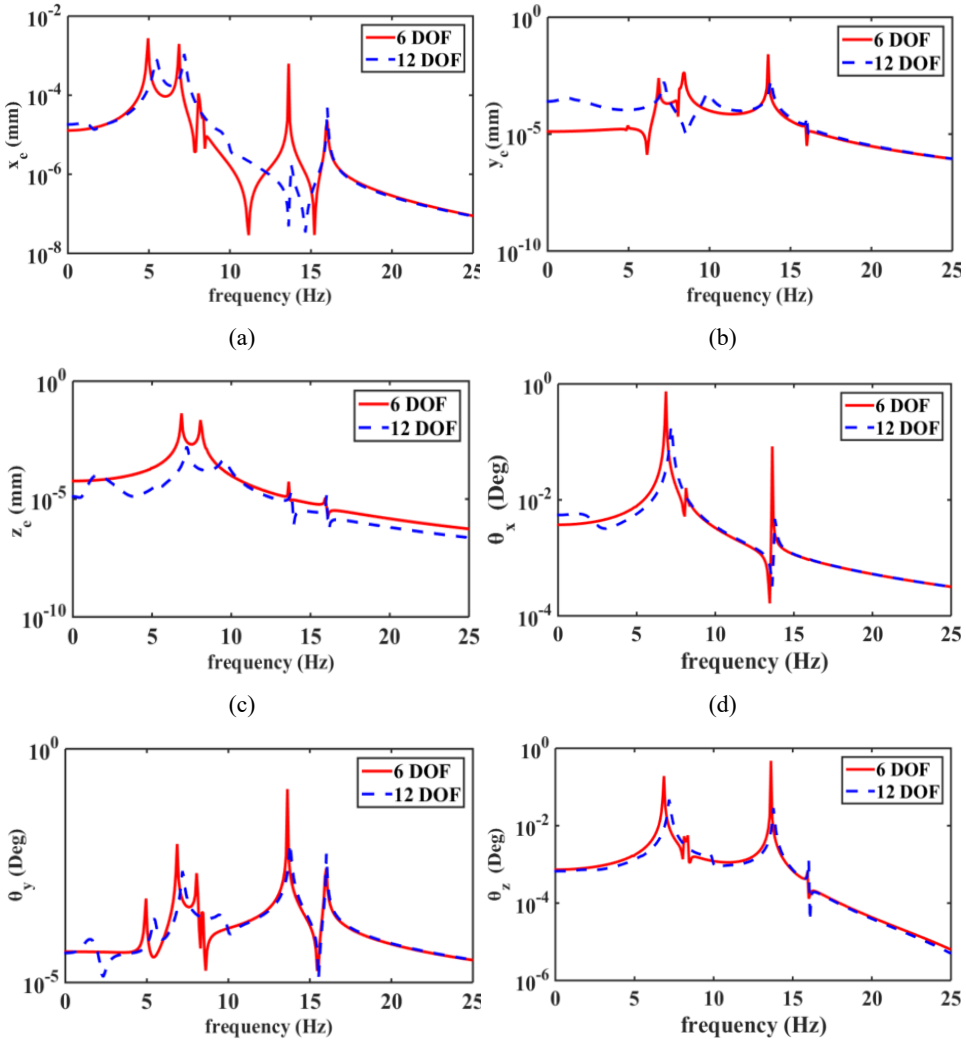

Figure 5 shows the variation of powertrain displacement response for the same Y-direction excitation. As can be seen in Figure 5, the difference in frequency response between the 12-degree-of-freedom and 6-degree-of-freedom mount systems considering the vehicle frame is significant at below 5 Hz. The difference is due to the influence of the natural frequency of the vehicle frame (between 1 Hz and 3 Hz). Therefore, for the decoupling analysis of the powertrain mount system, it is necessary to take the elastic base vehicle frame into account.

4 Optimisation of 12-degree-of-freedom mount system

4.1 Vehicle frame vibration response

The Laplace transform of equation (21) solves for the displacement response of the powertrain and vehicle frame as follows:

$$\begin{Bmatrix} q^e \\ q^c \end{Bmatrix} = \begin{bmatrix} K^e + iC^e - \omega^2 M_e & -K^{e\to c} - i\omega C^{e\to c} \\ -K^{c\to e} - i\omega C^{c\to e} & K^c + K^{c1} + i\omega C^c + i\omega C^{c1} - \omega^2 M_c \end{bmatrix}^{-1} \begin{Bmatrix} f^e \\ f^c \end{Bmatrix} \tag{30}$$

To rearrange equation (30), equation (31) is obtained.

$$\begin{aligned} &\begin{bmatrix} I & A_1 \\ A_2 & I \end{bmatrix} \begin{Bmatrix} q^e \\ q^c \end{Bmatrix} = \begin{Bmatrix} \left(K^e + iC^e - \omega^2 M_e\right)^{-1} f^e \\ \left(K^c + K^{cl} + i\omega C^c + i\omega C^{cl} - \omega^2 M_c\right)^{-1} f^c \end{Bmatrix} \\ &A_1 = -\left(K^e + iC^e - \omega^2 M_e\right)\left(K^{e\to c} + i\omega C^{e\to c}\right) \\ &A_2 = -\left(K^c + K^{cl} + i\omega C^c + i\omega C^{c1} - \omega^2 M_c\right)\left(K^{c\to e} + i\omega C^{c\to e}\right) \end{aligned} \tag{31}$$

Bessac et al. (1996) assumed a complete decoupling of the 12-degree-of-freedom mount system. The displacement of the powertrain when the engine alone is excited $q_0^e = (K^e - iC^e - \omega^2 M_e)^{-1} f_e$ and the displacement of the centre-of-mass of the vehicle frame when the road alone is excited $q_0^c = (K^c + K^{c1} + i\omega C^c + i\omega C^{c1} - \omega^2 M_c)^{-1} f^c$ can be obtained. Thus, equation (31) can be organised into equation (32). where q^e and q^c are the powertrain displacement and the vehicle frame centre-of-mass displacement of the 12-degree-of-freedom mount system. Here the matrix D is the coupling matrix between the powertrain and the vehicle frame of the 12-degree-of-freedom mount system (Hu and Singh, 2012).

$$\begin{Bmatrix} q^e \\ q^c \end{Bmatrix} = (1 - D)^{-1} \begin{Bmatrix} q_0^e \\ q_0^e \end{Bmatrix} \tag{32}$$

where the coupling matrix D is represented as follows.

$$D = \begin{bmatrix} 0 & A_1 \\ A_2 & 0 \end{bmatrix} \tag{33}$$

A sufficient condition for equation (32) to have a solution is that the matrix $(I - D)$ is invertible. Combining the data provided in Tables 1–4, solve for the spectral radius $P(D)$ of the coupling matrix. Figure 6 shows the spectral radius of the solved coupling matrix D. The coupling matrix has a spectral radius $P(D) > 1$ only within the natural frequency range of the vehicle frame and powertrain mount. The spectral radius of the coupling matrix $P(D) < 1$, is greater than the natural frequency range of the vehicle frame and powertrain mount. Again, since $P(D) \le \|D\| < 1$, the coupling matrix $(I - D)$ is non-singular. So, the approximate solution of the powertrain and vehicle frame displacement response can be obtained as follows:

$$\begin{Bmatrix} q^e \\ q^c \end{Bmatrix} \approx \sum_{n=0}^{N} D^n \begin{Bmatrix} q_0^e \\ q_0^c \end{Bmatrix} \tag{34}$$

Figure 6 Spectral radius of the coupling matrix of the 12-degree-of-freedom mount system (see online version for colours)

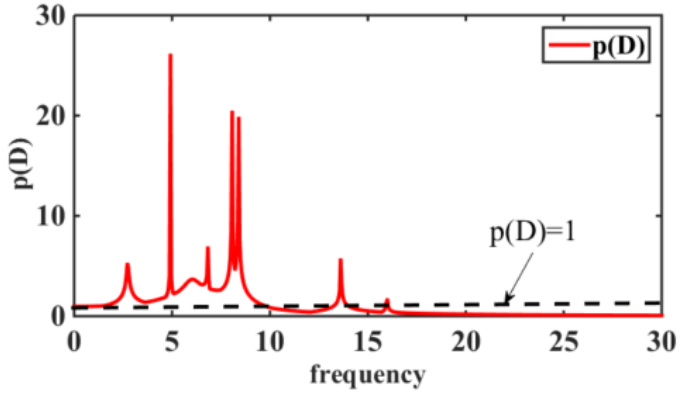

In this study, only engine excitation is considered and no road excitation is considered. Therefore, the displacement response $q_0^c = 0$ of the vehicle frame when the 12-degree-of-freedom mount system is completely decoupled. Thus, the vehicle frame displacement response expressed by the coupling matrix under engine excitation is derived as follows:

$$q^c = \sum_{n=0}^{N} D^n q_0^e \tag{35}$$

When the engine is excited around 100 N/m in the Y-direction, the displacement response of the vehicle frame vibration at $n = 2$ and $n = 100$ can be solved according to equation (35), as shown in Figure 7. As can be seen from Figure 7, the displacement response of vehicle frame vibration is almost the same when $n = 2$ and $n = 100$. For calculation simplicity, $n = 2$ is chosen to get the vehicle frame vibration displacement response. As a result, the vehicle frame vibration displacement response q^c can be obtained, and its equation (36) is shown.

$$q^c = I + D + D^2 \tag{36}$$

4.2 12-degree-of-freedom mount system optimisation

The optimisation of the mount system is to achieve an increased degree of decoupling in the direction of excitation force action and a reasonable configuration of the modal frequency. To this purpose, the vibration displacement response of the powertrain and vehicle frame are reduced and the vibration isolation performance of the system is improved. In the following, the objective function design, the selection of design variables, the setting of constraints, and the selection of optimisation algorithms are described.

Figure 7 Displacement response of $n = 2$ and $n = 100$ vehicle frame vibration, (a) X-direction (b) Y-direction (c) Z-direction (d) θ_{xc} direction (e) θ_{yc} direction (f) θ_{zc} direction (see online version for colours)

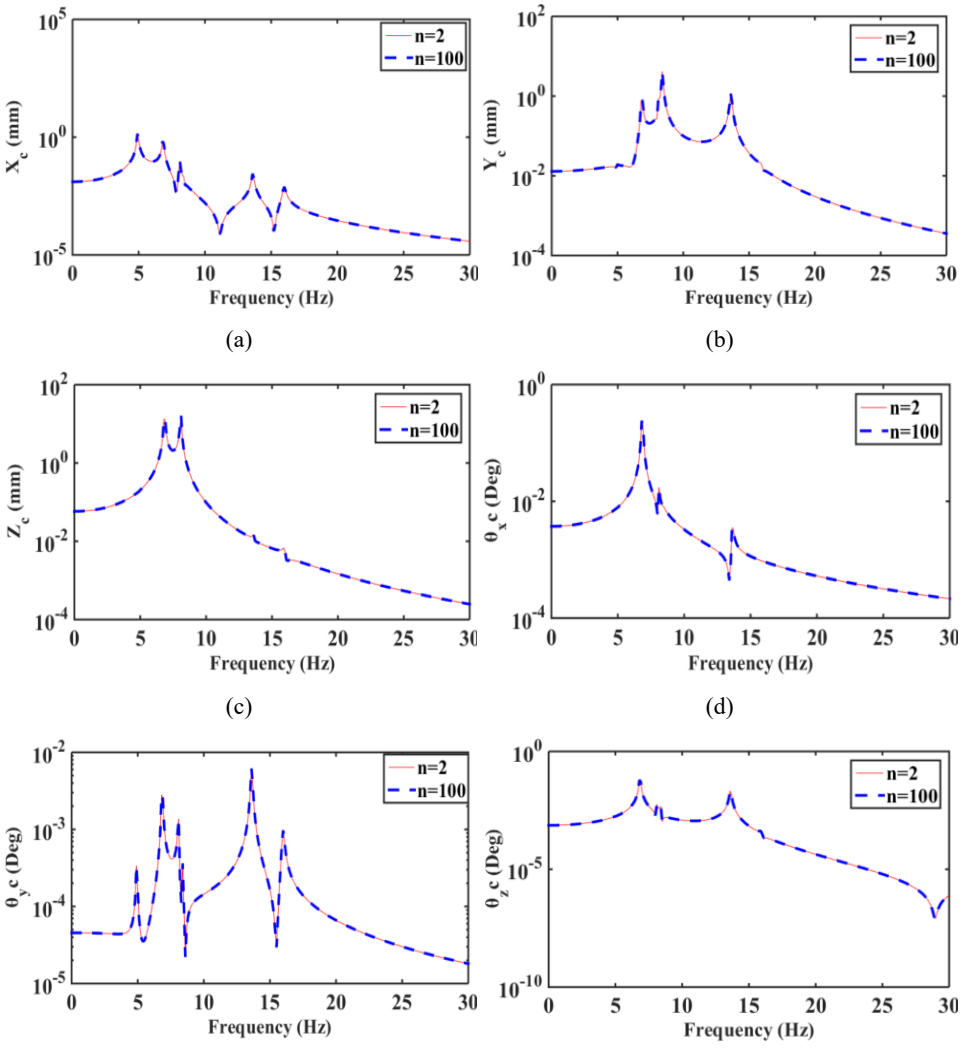

4.2.1 Design of the objective function

The object of this study is for a four-cylinder engine with the maximum 6th order decoupling rate of the powertrain and the vehicle frame vibration displacement response as the objective function. The specific objective function is designed with the following equation.

$$\begin{aligned} MinF_1(x) &= 6 - \left(T_x^e + T_y^e + T_z^e + T_{\theta x}^e + T_{\theta y}^e + T_{\theta z}^e\right) \\ MinF_2(x) &= q^c \end{aligned} \tag{37}$$

In the equation, $T_x^e, T_y^e, T_z^e, T_{\theta x}^e, T_{\theta y}^e, T_{\theta z}^e$ are the decoupling rates of the 6th order vibration of the powertrain of the 12-degree-of-freedom mount system considering the influence of the vehicle frame, q^c the body displacement response.

4.2.2 Design variables

Changes in both the stiffness of the mounts and the installation position result in changes in the value of the objective function. Therefore, the stiffness and mounting position of each mount is selected as the design, while the number of mounts $n = 3$ in this research. The selection of specific design variables stiffness and installation position parameters are shown below.

- Left mount: $1{,}080.1 < x_1 < 1{,}100.1$, $-160.2 < y_1 < -140.2$, $262.4 < z_1 < 282.4$.
- Right mount: $1{,}973.4 < x_2 < 1{,}993.4$, $-82.7 < y_2 < -62.7$, $327.6 < z_2 < 347.6$.
- Rear mount: $1{,}339.5 < x_3 < 1{,}359.5$, $164.1 < y_3 < 184.1$, $-124.1 < z_3 < -104.1$.
- Left mount: $28 < K_{u1}$ $52{,}112 < K_{v1} < 208$, $109.2 < K_{w1} < 202.8$.
- Right mount: $59.5 < K_{u2} < 110.5$, $116.2 < K_{v2} < 215.8$, $73.5 < K_{w2} < 136.5$.
- Rear mount: $27.3 < K_{u3} < 50.7$, $123.2 < K_{v3} < 228.8$, $117.6 < K_{w3} < 218.4$.

4.2.3 Constraints

The subject of this paper is a four-cylinder engine which has an idle speed of 750 r/min. The excitation frequency at idle speed can be calculated to be 25 Hz, so the natural frequency around the crankshaft direction is less than 12 times of the idle excitation (Yu et al., 2001; Endur and Tun, 2020). Therefore, the natural frequency around the crankshaft direction is less than 17 Hz. At the same time, each order of the powertrain mount system should avoid the vehicle rigid frame mode (1–3 Hz) and the under-spring mass jump frequency (15–18 Hz). Therefore, the modal range of the first six orders of the 12-degree-of-freedom mount system is controlled between 5 and 15 Hz (Alzahabi et al., 2003). At the same time, the order frequencies cannot overlap with each other. Therefore, the interval between the modal frequencies is controlled to be more than 1 Hz.

In summary, the mathematical model for the decoupling optimisation of the 12-degree-of-freedom mount system is obtained as follows:

$$MinF_1(x) = 6 - \left(T_x^e + T_y^e + T_z^e + T_{\theta x}^e + T_{\theta y}^e + T_{\theta z}^e\right)$$

$$MinF_2(x) = q^c$$

$$\text{s.t.} \quad 5\ Hz < f_i < 15\ Hz\ i = x, y, z, \theta_x, \theta_y, \theta_z$$

4.2.4 Optimisation method

Genetic algorithms (Deb, 2001) are computational models of biological evolutionary processes that simulate the mechanisms of natural selection and genetics. It has the advantage of fast convergence for multi-objective optimisation problems. The 12-degree-of-freedom mount system objective function is optimised for the design variables in the following steps.

1 Preparation of computational procedures for solving the decoupling rate and the natural frequency of the 12-degree-of-freedom system and the vehicle frame vibration displacement response.

2 Setting of input and output variables, constraints, optimisation objectives, and optimisation algorithms in the software.

3 NSGA-II is selected as the optimisation algorithm to obtain the maximum value of the 6th order decoupling rate of the powertrain and the minimum value of the vehicle frame vibration displacement response.

The initial population size N = 100, the number of iterations G = 500, the crossover probability P_c = 0.9, the variation probability P_m = 0.5, and the distribution indices of crossover and variation n_c = 20 and n_m = 20, respectively, were chosen for the run. The main cycle of NSGA-II is shown in Figure 8.

Figure 8 Flow charts of NSGA-II's main cycle section

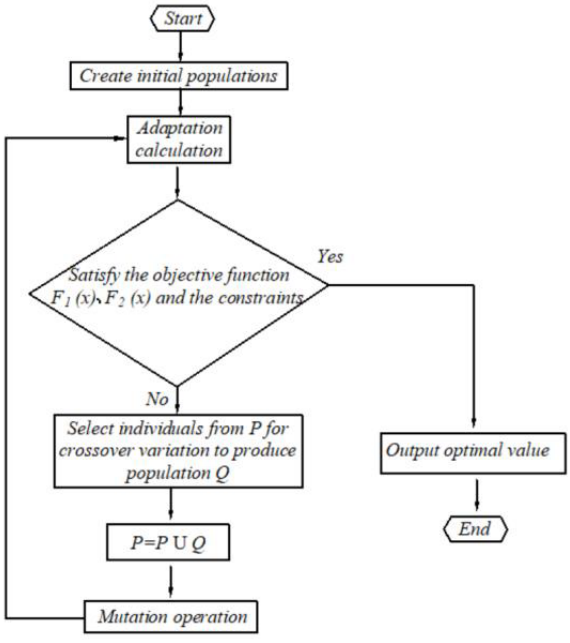

4.3 Analysis of optimisation results

From Figure 9, the decoupling rate in the foreaft direction improves from 79.99% to 80.505%; decoupling rate in the lateral direction from 61.745% to 70.594; bounce direction decoupling rate from 69.463% to 70.438%; similarly, the decoupling rate in the roll direction increased from the original 88.927% to 90.013%; the decoupling rate in the pitch direction is improved from 93.902% to 98.017%; in the Yaw direction the decoupling rate is improved from 77.445% to 95.407%. Since the 12-degree-of-freedom mount system involves coupling between the powertrain and the vehicle frame, there is more severe coupling in the lateral and bounce directions. However, the

12-degree-of-freedom mount system based on the multi-objective genetic algorithm was improved in all orders of decoupling rate.

Figure 9 Comparison of decoupling rate of each order of mounts before and after optimisation (see online version for colours)

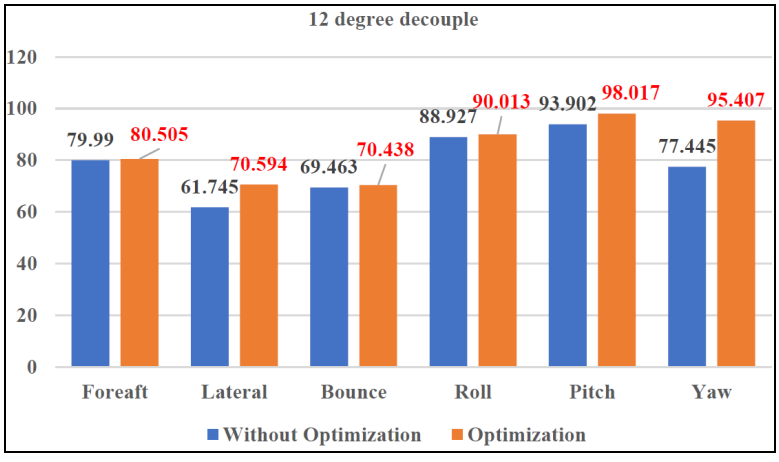

Figure 10 shows the optimised and unoptimised powertrain centre-of-mass displacement responses using the multi-objective genetic algorithm. From Figure 10, it can be seen that the centre-of-mass displacement of the powertrain is decreasing after optimisation. Figure 10 shows that the displacement of the centre-of-mass of the powertrain between 0–5 Hz is poorly optimised in the Y-direction and θ_{ye} direction, which is mainly due to the resonance of the natural frequency of the vehicle frame within 5 Hz and the coupling between the powertrain and the vehicle frame.

Figure 11 shows the displacement response of the vehicle frame centre-of-mass considering the engine torque direction excitation. The red solid line is the unoptimised vehicle frame centre-of-mass displacement response, and the green dashed line is the vehicle frame centre-of-mass displacement response curve optimised by a multi-objective genetic algorithm. As can be seen from Figure 11, resonance with the vehicle frame natural frequency in the low frequency region 0–5 Hz is less effective in the Y, Z and around Z directions. However, the displacements of the centre-of-mass of the vehicle frame larger than 5 Hz were all better improved after optimisation. It can be seen that the optimisation method is applicable to the optimal design of decoupling the 12-degree-of-freedom mount system considering the influence of the vehicle frame.

This section explores and investigates the basic requirements for the optimisation of 12-degree-of-freedom mount system. A multi-objective genetic algorithm is used to improve the first sixth order decoupling rate of the mount system and minimise the vehicle frame centre-of-mass displacement response as the optimisation objectives, using the mount stiffness and installation position as design variables. The optimised 12-degree-of-freedom mount has improved the decoupling rate of each order and reduced the displacement of the vehicle frame centre-of-mass, which has laid a theoretical foundation for achieving the vibration isolation requirements of the mount system.

Figure 10 Comparison of displacement response of optimised and unoptimised powertrain centre-of-mass, (a) displacement in X-direction (b) displacement in Y-direction (c) displacement in Z-direction (d) displacement in θ_{xe} direction (e) displacement in θ_{ye} direction (f) displacement in θ_{ze} direction (see online version for colours)

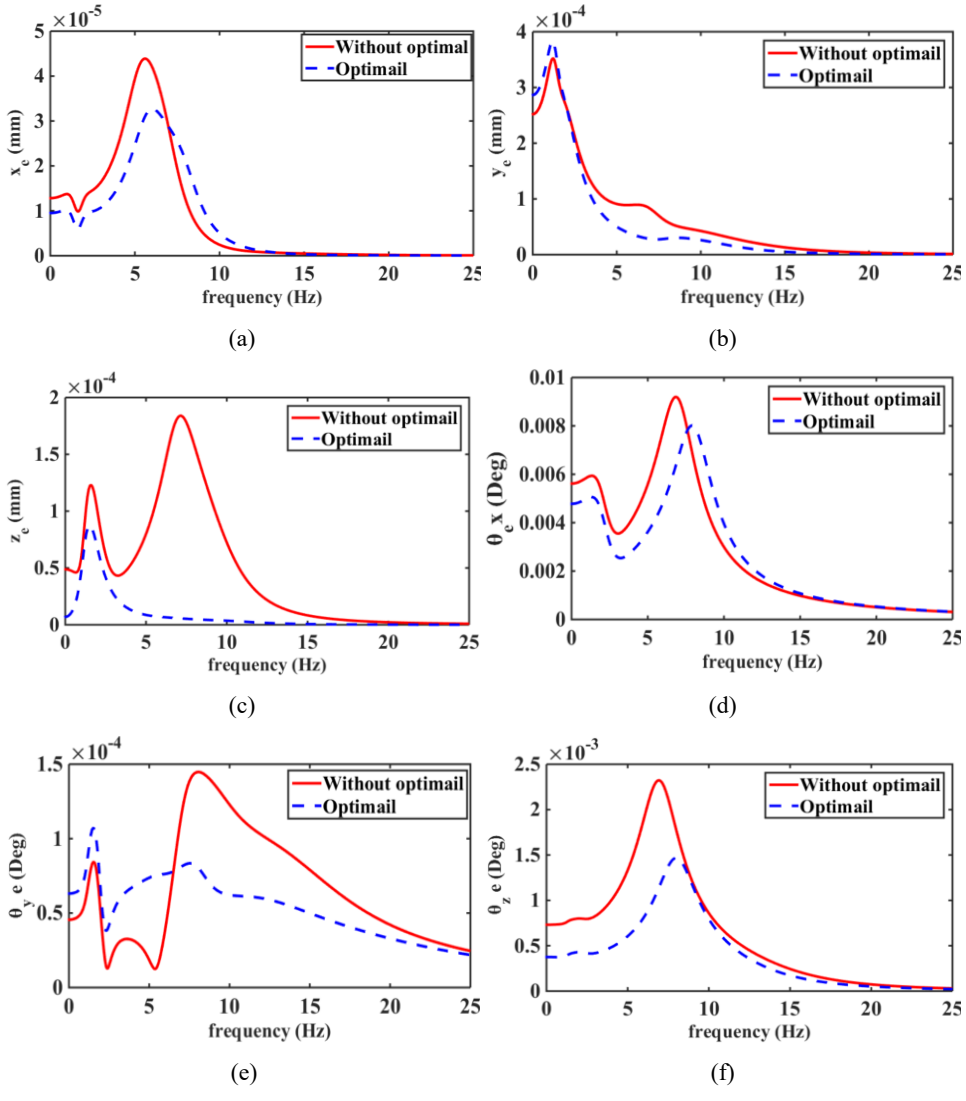

5 Conclusions

In this paper, the 12-degree-of-freedom mount system is decoupling and optimised considering the interaction effect between the powertrain and the vehicle frame.

1 Derive the equations of motion for 6 and 12 degrees of freedom, respectively, and solve for their natural frequencies and displacement responses to verify the necessity of decoupling the 12-degree-of-freedom mount system.

2 Use a multi-objective genetic algorithm to decouple and optimise the design of a 12-degree-of-freedom mount system, which effectively improves the decoupling rate of the mount system and reduces the displacement response of powertrain and vehicle frame, and improves the vibration isolation performance of the system.

Figure 11 Comparison of displacement response of optimised and unoptimised vehicle frame, (a) displacement in X-direction (b) displacement in Y-direction (c) displacement in Z-direction (d) displacement in θ_{xc} direction (e) displacement in θ_{yc} direction (f) displacement in θ_{zc} direction (see online version for colours)

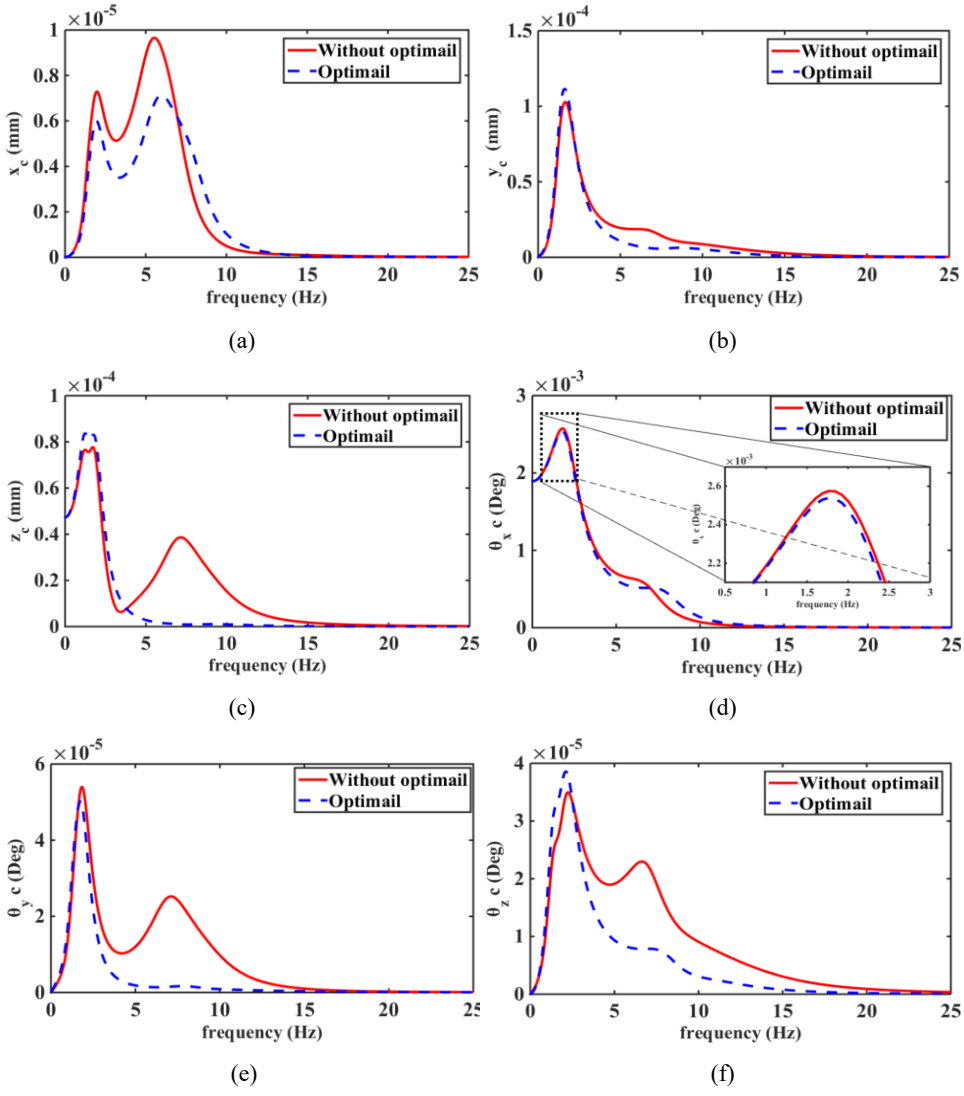

References

Alzahabi, B., Mazzei, A. and Natarajan, L.K. (2003) 'Investigation of powertrain rigid body modes', in *Conference and Exposition on Structural Dynamics Proceedings*, Florida, 3–6 February.

Bessac, F., Gagliardini, L. and Guyader, J.L. (1996) 'Coupling eigenvalues and eigenvectors: a tool for investigating the vibroacoustic behaviour of coupled vibrating systems', *Journal of Sound & Vibration*, Vol. 191, No. 5, pp.881–899.

Colgate, J.E., Chang, C.T. and Chiou, Y.C. (1995) 'Modeling of hydraulic engine mount focusing on response to sinusoidal and composite excitations', *Journal of Sound and Vibration*, Vol. 184, No. 3, pp.503–528.

Dai, F., Wu, W. and Wang, H. (2013) 'Study on mount matching optimization for removing powertrain abnormal low frequency vibration', *Lecture Notes in Electrical Engineering*.

Deb, K. (2001) *Multi-Objective Optimization using Evolutionary Algorithms*, Wiley, Hoboken.

Endur, P. and Tun, B. (2020) 'Design sensitivity and optimization of powertrain mount system design parameters for rigid body modes and kinetic energy distributions', *Journal of the Brazilian Society of Mechanical Fences and Engineering*, Vol. 42, No. 9, pp.1–16.

Erdelyi, H.E., Roesems, D. and Toso, A. (2013) *Powertrain Mounting System Layout for Decoupling Rigid-Body Modes in the Vehicle Concept Design Stage*, SAE 2013 World Congress & Exhibition.

Hu, J.F. and Singh, R. (2012) 'Improved torque roll axis decoupling axiom for a powertrain mounting system in the presence of a compliant base', *Journal of Sound & Vibration*, Vol. 331, No. 7, pp.1498–1518.

Jeong, T. (2000) *Analysis of Powertrain Mounts with Focus on Torque Roll Axis De-coupling and Frequency-Dependent Properties*, The Ohio State University.

Lee, J.M., Yim, H.J. and Kim, J.H. (1995) *Flexible Chassis Effects on Dynamic Response of Engine Mount Systems*, SAE Technical Paper Series, 951094.

Lee, K.H. and Choi, Y.T. (1991) *Performance Design of Hydraulic Mount for Low Frequency Engine Vibration and Noise Control*, SAE Technical Paper Series, No. 941777.

Mahil, A. and Faris, W.F. (2014) 'Modelling and control of four and six DOF active engine mount system using (PID and LQR)', *International Journal of Vehicle Noise & Vibration*, Vol. 10, No. 4, p.326.

Michael, M. (1994) *Methods for the Reduction of Noise and Vibration in Vehicles Using an Appropriate Engine Mount System*, SAE Paper, No. 942414.

Mita, T. and Ushijima, T. (1986) 'Current review of vibration-insulating rubber products for automobiles', *J. Soc. Autom. Eng. Jpn*., Vol. 40, No. 5, pp.1288–1296.

Park, J.Y. and Singh, R. (2007) *Effect of Engine Mount Damping on the Torque Roll Axis Decoupling*, SAE Technical Papers.

Qatu, M.S. (2012) 'Recent research on vehicle noise and vibration', *International Journal of Vehicle Noise and Vibration*, Vol. 8, No. 4, pp.289–301.

Rivin, E.I. (1985) *Passive Engine Mounts-Some Directions for Further Development*, SAE International Congress and Exposition.

Sun, Y.H. and Jin, G.C. (2012) 'Optimization for powertrain mounting system based on theory of energy decoupling', *Advanced Materials Research*, Vol. 421, No. 1, pp.203–207.

Swanson, D.A. (1993) *Active Engine Mounts for Vehicles*, SAE Technical Paper Series, 932432, USA.

Takano, U.T. and Kojima, K. (1988) *High Performance Hydraulic Mount for Improving Vehicle Noise and Vibration*, SAE Paper, No. 880073.

Wang, X. (2010) *Vehicle Noise and Vibration Refinement*, CRC Press, Woodhead Publishing Limited.

Wu, J., Liu, X. and Shan, Y. (2018) 'Robustness optimization of engine mounting system based on Six Sigma and torque roll axis decoupling method', *Proceedings of the Institution of Mechanical Engineers Part D Journal of Automobile Engineering*, DOI: 095440701875524.

Yoon, J.Y. and Singh, R. (2011) 'Estimation of interfacial forces in a multi-degree of freedom isolation system using a dynamic load sensing mount and quasi-linear models', *Journal of Sound and Vibration*, Vol. 330, Nos. 18–19, pp.4429–4446.

Yu, Y., Naganathan, N.G. and Dukkipati, R.V. (2001) 'A literature review of automotive vehicle engine mounting systems', *Mech. Mach. Theory*, Vol. 36, No. 1, pp 123–142.